Protonation of benzo[*a*]pyrene, dibenzo[*a*,*e*]pyrene and benzo[*e*]pyrene in superacids: NMR studies of charge distribution in persistent arenium ions and AM1 calculations

Kenneth K. Laali,*[a] Poul Erik Hansen,[b] John J. Houser[c] and Maximilian Zander[d]

[a] *Department of Chemistry, Kent State University, Kent, OH 44242, USA*
[b] *Department of Life Sciences and Chemistry, Roskilde University, DK-4000 Roskilde, Denmark*
[c] *Department of Chemistry, University of Akron, Akron, OH 44325, USA*
[d] *Rütgerswerke AG, D-44558 Castrop-Rauxel, Germany*

Benzo[*a*]pyrene **1** and dibenzo[*a*,*e*]pyrene **2** are monoprotonated with FSO_3H–SO_2ClF to give persistent arenium ions of protonation at C-6 ($\mathbf{1H^+}$) and C-8 ($\mathbf{2H^+}$), respectively. The low temperature protonation of benzo[*e*]pyrene **3** under a variety of conditions produced a mixture of arenium ions of attack at C-1 ($\mathbf{3aH^+}$) and C-3 ($\mathbf{3bH^+}$).

The charge distribution pattern in the resulting arenium ions (as probed by low temperature ^{13}C and ^1H NMR spectroscopy) remains very much analogous to those of alkyl(cycloalkyl)pyrenes, showing significant phenalenium ion character (predominant charge alternation at the periphery of the pyrene moiety).

The arenium ion energies and charges were examined by semiempirical theory (AM1). For **1**, in agreement with experiment, protonation at C-6 is most favoured and the changes in charge distribution ΔQ [q_c(ion) − q_c(neutral)] indicated a very distinct phenalenium unit. Attack at other sites is less favoured, with that at C-2 being least likely. The extent of positive charge delocalisation becomes more limited as the arenium ion energies increase.

In accord with experiment, AM1 calculations indicate that for **2**, the arenium ion of protonation at C-8 is the most stable followed by those of C-1 and C-3 which are 4.5 and 5.1 kcal mol^{-1} less stable. Charge delocalisation away from the protonation site in these cations is predicted to be more extensive and involve a phenalenium moiety.

For **3**, in line with experiment, the arenium ion energies for attack at C-1 and C-3 are almost identical and most favoured.

The results indicate that despite the pronounced effect that benzannellation has on carcinogenicity, the preferred site(s) of electrophilic attack are those which lead to the most highly delocalised carbocations. Among these, formation of a robust phenalenium ion moiety is always favoured. Possible implications of these findings in relation to carcinogenesis models mediated by arenium ions are discussed.

The oxidation dications of **1**–**2** were also probed by the AM1 method.

Introduction

As an environmental pollutant and a potent carcinogen, benzo[*a*]pyrene **1** (Fig. 1) has been the focus of numerous experimental and theoretical studies which have contributed to the development of bay-region theory.[1–4]

Unlike **1**, the isomeric benzo[*e*]pyrene **3** is not carcinogenic. The carcinogenicities of dibenzopyrenes vary depending on the mode of annellation. Thus, whereas dibenzo[*a*,*e*]pyrene **2** is mildly carcinogenic, dibenzo[*a*,*l*]pyrene **4** is very potent.[5]

The critical intermediates that ultimately form PAH–DNA adducts are either the diol epoxides or the radical cations RCs formed by one-electron oxidation (or both).[6,7]

Kinetic and solvolytic studies on various K-region arene oxides of PAHs have provided ample evidence that ring opening to benzylic carbocations occurs. Substituent effect studies on reaction rate yield large negative ρ values indicative of carbocationic transition states.[8–10] Binding to DNA either *via* an S_N1 process or by S_N2 mechanism with an unsymmetrical transition state with partial positive charge development on the aromatic moiety has been proposed.[9]

For benzo[*a*]pyrene, carbocations may be formed directly *via* attack of electrophilic oxygen (from the hydroxylase system) followed by nucleophilic attack by nucleotides at the remote sites.[11]

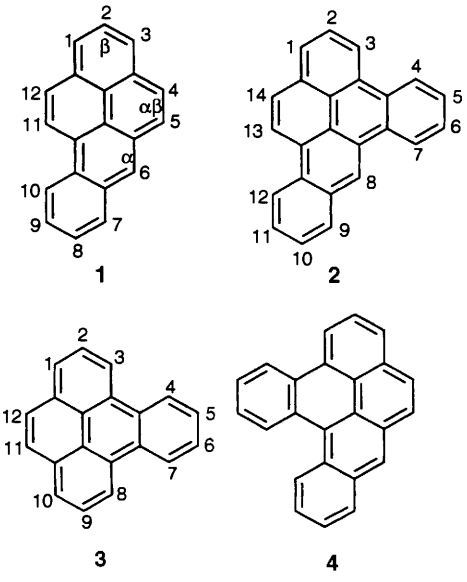

Fig. 1 Benzo[*a*]pyrene **1**, dibenzo[*a*,*e*]pyrene **2**, benzo[*e*]pyrene **3** and dibenzo[*a*,*l*]pyrene **4**

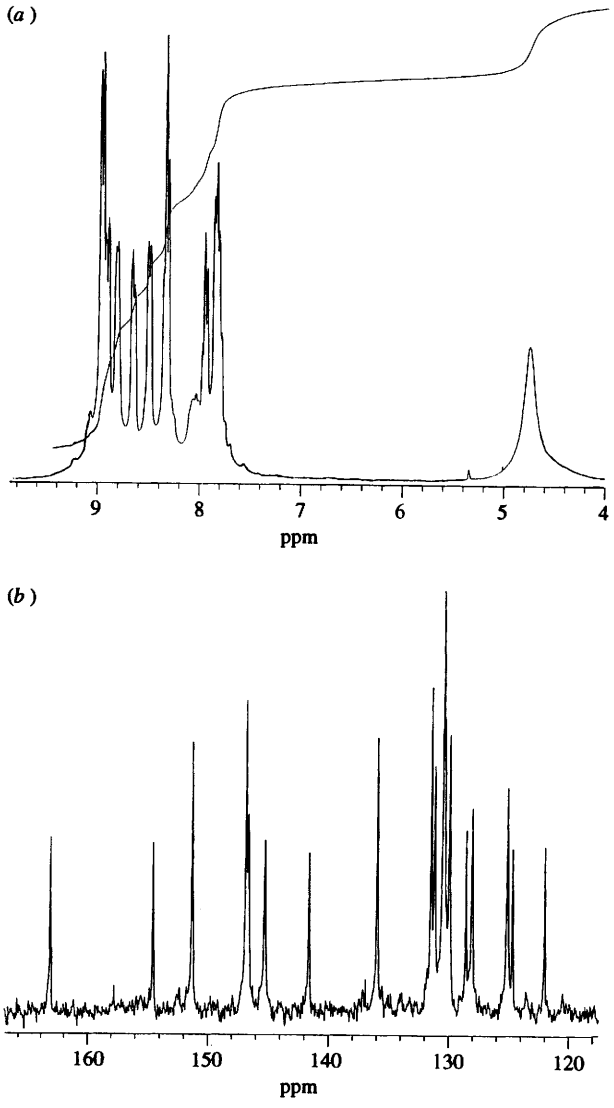

Fig. 2 (*a*) ^{1}H NMR spectrum of $1H^+$; (*b*) the aromatic region of ^{13}C NMR spectrum $1H^+$

Since the more extensively delocalised carbocations produced metabolically are more likely to undergo nucleophilic attack by nucleotides at remote sites, we reasoned that charge delocalisation mapping of the arenium ions of various classes of fused PAHs (both carcinogenic and non-carcinogenic) might be helpful in establishing whether there is a correlation between certain specific charge delocalisation pathways and carcinogenicity.

From the absorption spectra of various PAHs in HF, Dallinga *et al.*[12] predicted in the late 1950s that **1** is protonated at C-6 and that **3** gives a mixture of two arenium ions of α attack.

Early in the development of NMR studies in strong acids, a 40 MHz ^{1}H NMR spectrum of the conjugate acid of **1** in TFA-H_2O-BF_3 solvent was reported by MacLean *et al.* with the CH_2^+ at 3.27 ppm.[13,14]

A previous ^{1}H NMR study[15] of H–D exchange (D_2SO_4, RT) on **1** demonstrated that H-6 exchanged most rapidly. Hitherto no high-field NMR studies on persistent arenium ions of **1–3** have appeared.

In continuation of our previous studies on arenium ions and oxidation dications of PAHs,[16–23] we report a protonation study on **1–3**. Our goal was to determine whether benz-annellation changes the preferred site of electrophilic attack and/or the mode of charge delocalisation.

Chart 1

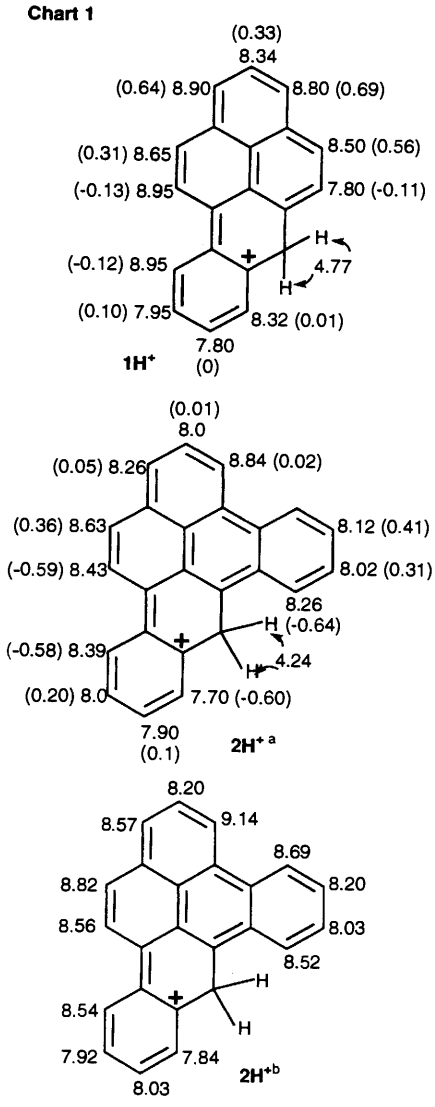

[a] Protonation effects are given in parentheses. [b] More concentrated ion solution prepared for 2D NMR studies.

Chart 1 ^{1}H NMR assignments for the arenium ions

Results and discussion

NMR spectra of the substrates

The ^{1}H and ^{13}C NMR spectra of **1** have been unambiguously assigned before by London *et al.*[24] The H-10/H-11 bay region protons are the most deshielded. There is a distinct singlet at 8.54 ppm for H-6. The C-13 resonances occur in a narrow range between 131.6–122.18 ppm.

The significant feature of the ^{1}H NMR spectrum of **2**[25] is the highly deshielded nature of the bay region singlet (H-8 at 9.20 ppm), followed by the bay region H-12 and H-13 (8.97 and 9.02 ppm).

The poor solubility of **2** in $CDCl_3$ prevents full analysis of its ^{13}C NMR spectrum. Whereas the H-bearing carbons are all discernible (between 129.09–120.2 ppm), some of the ring junction carbons are obscured (Chart 2).

For **3**, both the ^{1}H and ^{13}C NMR spectra have been previously reported[26] but specific assignments are not given.

Superacid protonations

(a) Benzo*(a)*pyrene (1). Careful addition of cold FSO_3H–SO_2ClF to a slurry of **1** in SO_2ClF at −78 °C cleanly produced the monoarenium ion $1H^+$. The ^{1}H and the aromatic region of

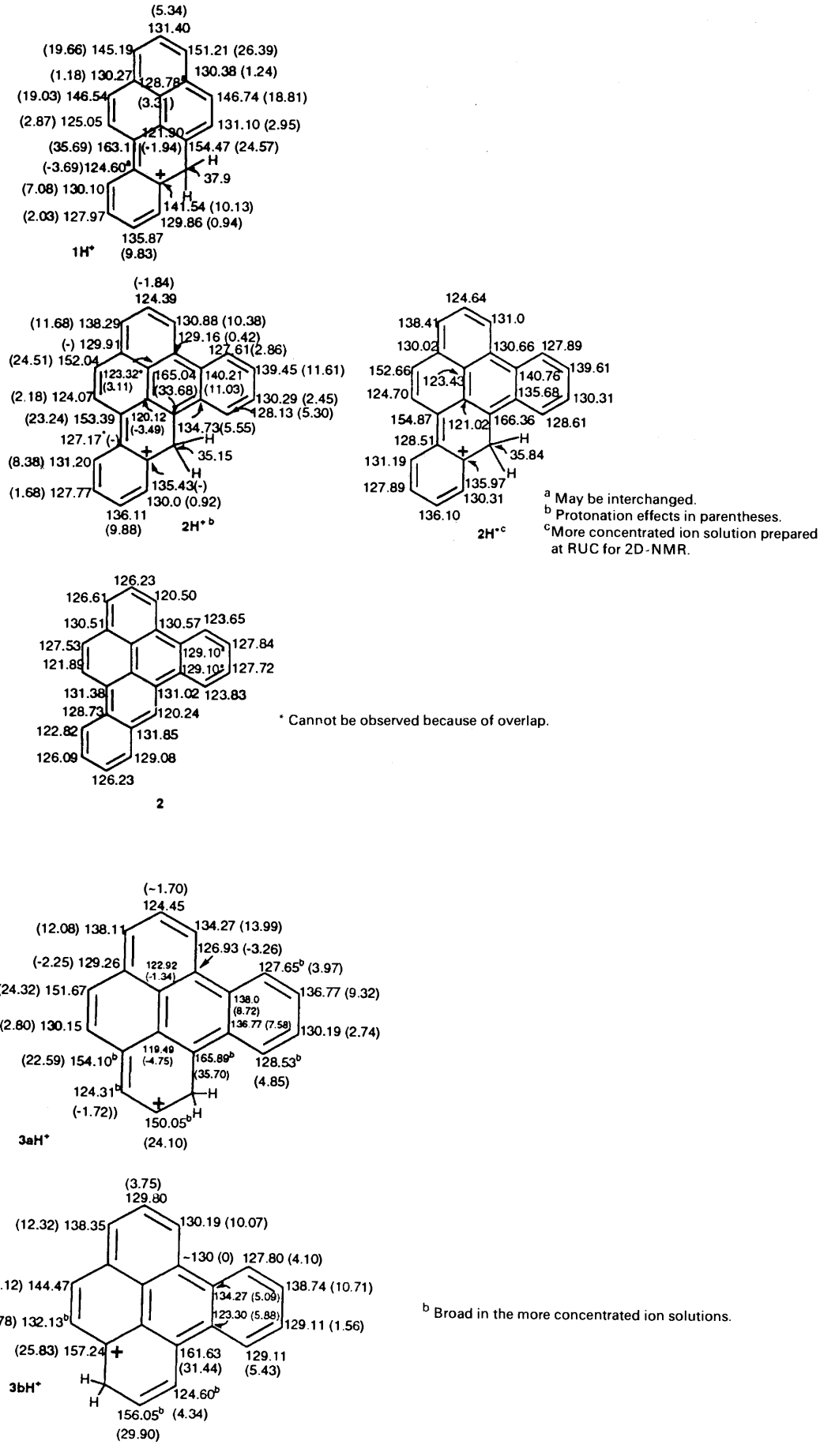

[a] May be interchanged.
[b] Protonation effects in parentheses.
[c] More concentrated ion solution prepared at RUC for 2D-NMR.

* Cannot be observed because of overlap.

[b] Broad in the more concentrated ion solutions.

Chart 2 ^{13}C NMR assignments for the arenium ions (^{13}C NMR data for **2** itself is also shown)

^{13}C NMR spectra are displayed (Fig. 2) and the specific assignments are given (Charts 1, 2).

The ^{1}H assignments are based on chemical shifts, integrals, multiplicities (and coupling constants). Several low-field aromatic resonances overlap at 300 MHz. The diagnostic CH_2^+ is a broad singlet at 4.77 ppm. The most downfield doublet is assigned to H-10/H-11. Interestingly, H-1 is a doublet of doublets showing an unusually large vicinal coupling (8.7 Hz) in addition to a smaller long-range coupling (J = 1.9 Hz) probably to H-3.

The ^{13}C assignments (Chart 2) are based on the chemical shifts, C-H couplings in the coupled spectrum (one-bond and long-range), and the magnitude of $\Delta\delta$ values in comparison with other pyrenium ions we studied previously.[16–19,22,23] The expected 19 aromatic resonances are resolved (two coinciding). The two most deshielded aromatic carbon resonances at 163.1 and 154.4 ppm (both non-hydrogen bearing), are assigned to the '*para*' and '*ortho*' carbons; the CH_2^+ resonance is at 37.9 ppm.

(*b*) Dibenzo[*a*,*e*]pyrene (2). Monoprotonation of **2** was studied in three different media, namely FSO_3H–SO_2ClF, CF_3SO_3H 'TfOH'–SO_2ClF and FSO_3H·SbF_5 (4:1)–SO_2ClF. In all cases addition of the cold superacid system to the slurried substrate in SO_2ClF at −78 °C produced clear red solutions whose ^{1}H and ^{13}C NMR spectra indicated the formation of $\mathbf{2H}^+$ as the only NMR-detectable arenium ion.

The ^{1}H NMR spectra showed variable degrees of line-broadening and several overlapping resonances. In addition, the chemical shifts showed sensitivity to ion concentration and the extent of dilution with SO_2ClF. Samples prepared in higher concentrations for 2D-NMR studies were broader and showed variable chemical shifts for several resonances. Analysis of the ^{1}H NMR spectrum could be achieved with an H–H COSY spectrum.

In a control experiment a cold aliquot was transferred from the NMR tube to a quartz EPR tube and examined by EPR spectroscopy. A broad pseudo-septet was observed (g = 2.002 G). The resolution was not improved by exclusion of dissolved oxygen or by lowering the temperature. Therefore, the origin of broadening and chemical shift variations of the protons can be traced to the presence of radical cation RC ($\mathbf{2}^{\bullet+}$) in equilibrium with the arenium ion.

The more concentrated ion solutions are more likely to contain RC due to increased local overheating. We[18] and others[27] have shown that the RC of the PAHs with lower ionization potentials than **2** can still be detected by EPR spectroscopy; in such cases, without noticeable line-broadening in the NMR spectrum.

The ^{1}H NMR spectrum of $\mathbf{2H}^+$ (in FSO_3H–SO_2ClF solvent) [Fig. 3(*a*)] shows a singlet at 4.24 (2 H) for CH_2^+, triplets are seen at 7.90 and 8.00 ppm and with some overlap at 8.00, 8.11, and 8.12 ppm. The remaining resonances are doublets.

The significant features of the ^{1}H NMR spectrum are the absence of the H-8 singlet and the high-field shifts of the bay region protons. For H-7/H-9 this is understandable since rehybridisation at C-6 reduces buttressing. The lack of expected deshielding for other protons may be due to a reduced ring current in the larger $\mathbf{2H}^+$ as compared to $\mathbf{1H}^+$; assignments were fine-tuned by a COSY analysis (at 215 K).

The ^{13}C NMR spectrum of $\mathbf{2H}^+$ is well resolved and could be fully assigned based on the chemical-shift criteria and carbon–proton couplings (Chart 2). The aromatic region [Fig. 3(*b*)] exhibits all the expected 23 resonances (between 165.0–120.0 ppm). The CH_2^+ signal is at 35.1 ppm. Furthermore, presence of RC in the more concentrated solutions leads to a change in the chemical shifts for those protons which are close to the protonation site (Chart 2), but not to discernible line-broadening. It should also be noted that traces of CF_2HD

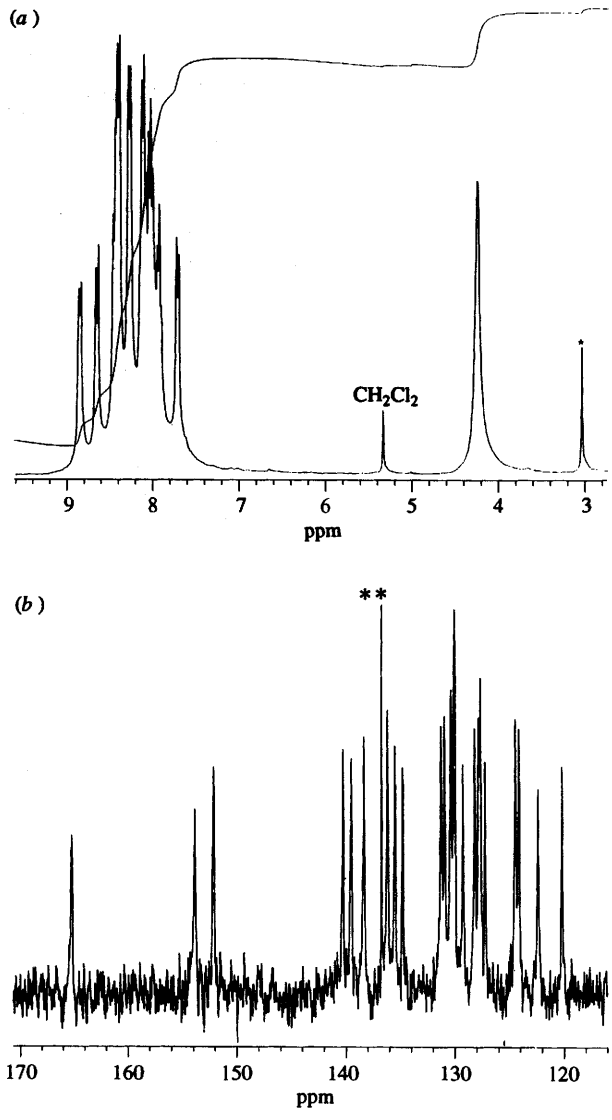

Fig. 3 (*a*) ^{1}H NMR spectrum of $\mathbf{2H}^+$; (*b*) the aromatic region of ^{13}C NMR spectrum of $\mathbf{2H}^+$

(formed *via* CD_2Cl_2 in the superacid)[18] were detectable in solution.†

Protonation of benzo[*e*]pyrene (3). Careful addition of FSO_3H–SO_2ClF to a slurry of **3** in SO_2ClF at −78 °C gave a clear red solution whose ^{1}H NMR spectrum [Fig. 4(*a*)] showed it to contain a mixture of two arenium ions $\mathbf{3aH}^+$ and $\mathbf{3bH}^+$ in an approximately 70:30 ratio.

The aliphatic region exhibited two CH_2^+ resonances at 4.11 (the more predominant) and 4.39 ppm. The broader, more upfield, resonance is assigned to CH_2^+ of $\mathbf{3aH}^+$ and the 4.39 ppm signal to the other cation. The aromatic resonances (appearing between 9 and 7 ppm) show very extensive overlap consistent with two structurally similar arenium ions.

Preparation of more concentrated ion solutions (for COSY work) led to broader proton resonances. Those at 4.11 and 4.39 merged and became broader (*ca.* 4.2 ppm); two additional broad resonances appeared around 7 ppm, which upon raising the temperature (from 203 to 233 K) merged and almost vanished

† Although the same ion could be generated in 'TfOH'–SO_2ClF, ^{13}C NMR studies in this medium are less useful owing to the presence of a strong CF_3 quartet of the solvent and close proximity of the latter to several upfield arenium-ion carbon resonances.

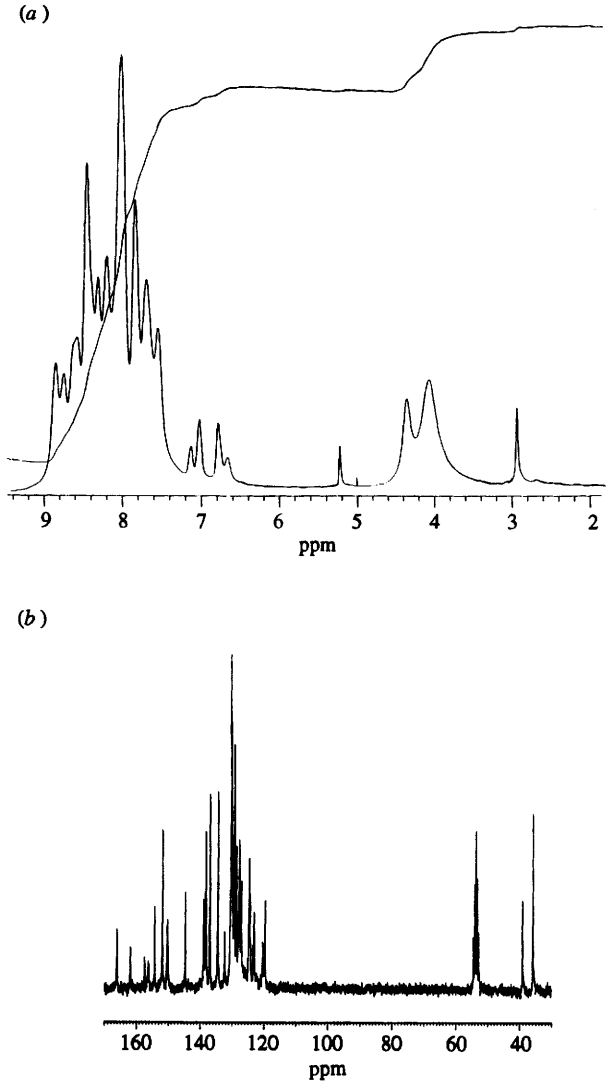

Fig. 4 (*a*) and (*b*) ^1H and ^{13}C (aromatic region) spectra of **3aH**$^+$ and **3bH**$^+$ mixture

into the baseline. The resonance at *ca.* 4.2 became broader and a shift of the aromatic absorptions to high frequencies was also noted.

The ^{13}C NMR spectrum [Fig. 4(*b*)] exhibits two CH_2^+ signals at 36.4 and 39.6 ppm. Again the more intense signal is more shielded, assigned to CH_2^+ of **3aH**$^+$.

The ^{13}C resonances (Chart 2) were assigned based on the chemical shifts and relative populations of the two isomers and in comparison with the structurally similar **2H**$^+$. Extensive line broadening was also seen in the carbon spectra which is thought to be due to RC formation. Interestingly, the line broadenings were found to be distance dependent; those at the proximity of the protonation site were broader. Thus for **3aH**$^+$, C-3a, C-12a, C-1, C-2 and C-4 resonances were clearly broader. For the two low-field-shifted quaternary carbons C-12a and C-3a, the broader one was assigned to C-12a which is closer to C-1. For **3bH**$^+$, line broadening, although less severe, was seen for C-2, C-3, C-12a and C-12. The latter supports the assignment of the minor isomer.

Attempts to increase the proportion of one isomer at the expense of the other by cold storage of the NMR samples or by raising temperature were unsuccessful.

AM1 calculations

By use of simple Hückel theory, Gold and Tye[28] correctly predicted (in 1952) that benzo[*a*]pyrene is protonated at C-6.

The energies of various arenium ions of **1** were later calculated by Dewar–PI calculations.[29]

We have calculated the arenium energies of **1** by the AM1 method. Fig. 5 shows the calculated $\Delta\Delta H_f^\circ$ of various cations (ΔH_f° for benzo[*a*]pyrene = 87.29 kcal mol^{-1}), and the magnitude of changes in charge distribution q_c(ion) − q_c(neutral) shown by dark (+) and light (−) circles.

Clearly, arenium ions of protonation at the α positions of the pyrene moiety are much more stable. Among these, attack at C-6 (**A**) has the lowest energy (152.8 kcal mol^{-1}), whereas arenium ion of β-protonation (**L**) is least stable (172.8 kcal mol^{-1}).

Charge delocalisation in A (and B, C) points to strong phenalenium ion character of these arenium ions, whereas other less stable arenium ions have more limited conjugation paths, which eventually become more or less restricted to the ring undergoing attack.

The ΔH_f° of **2** is calculated at 104.0 kcal mol^{-1}. Fig. 6 depicts the $\Delta\Delta H_f^\circ$ for various possible arenium ions and the ΔQ values (ion–neutral) for each cation. Protonation at C-8 is predicted to be the most favoured ($\Delta\Delta H_f^\circ$ = 154.1 kcal mol^{-1}), followed by those of C-1 and C-3 which are 4.5 and 5.1 kcal mol^{-1} less stable.

From the change in the AM1 charges it is apparent that arenium ions A, B, C show extensive charge alternation within a phenalenium unit. Benzannellation modulates the magnitude of positive charge accumulation in the α and αβ positions by dispersing charge into one or two conjugated carbon(s).

Comparison of the change in AM1 charges between B and C (Fig. 6) shows that carbon C-3a is always more positive than C-14a. In arenium ion D charge alternation is clearly predicted within a naphthalenium moiety extending up to three other conjugated carbons. Other arenium ions show limited conjugation paths.

The oxidation dication of **1** was generated by Forsyth and Olah[27] as part of an extensive survey of PAH dications. All the expected 20 carbon resonances were seen. The dication of **2** has not as yet been reported. To provide a comparison with **1H**$^+$ and **2H**$^+$ we calculated the charge delocalisation mode in **1**$^{2+}$ and **2**$^{2+}$ (Fig. 7). The ΔQ(ion–neutral) profiles show that as in the parent pyrenium dication and alkyl(cycloalkyl)pyrenium dications,[27,18] the α positions of the pyrene moiety in both systems sustain a large portion of the positive charge, followed by one αβ position and two carbons of the benzo[α] ring. The largest ΔQ is at C-6, consistent with the assignment of the most deshielded ^{13}C resonance at 186.0 ppm to C-6 of dication.[27] The benzo[*e*] ring of **2** does not contribute much to charge delocalisation.

The forms of the HOMO–LUMOs for **1**$^{2+}$ and **2**$^{2+}$ are depicted in Fig. 8 (calculated HOMO–LUMO gaps are 5.78 and 4.98 eV, respectively).

Although benzo[*e*]pyrene was included in a recent semi-empirical study,[30] relative arenium energies have apparently not been examined. The AM1 calculated $\Delta\Delta H_f^\circ$ values are displayed (Fig. 9).

Arenium ions of attack at the two α positions have near identical energies and are the most stable (AM1 calculated for ΔH_f for **3** is +83.85 kcal mol^{-1}) (lit.,[30] 83.99 kcal mol^{-1}). Comparing the delocalisation path for the most favoured arenium ions **A** and **B** (Fig. 9). reveals that the '*para*' positions (C-3a and C-14a, respectively) are always more positive than '*ortho*' positions. The phenalenium character although still apparent, has somewhat diminished compared with that of the energetically favoured arenium ions of **1** and **2**. Again, the degree of charge alternation at the periphery diminishes as the arenium ions become less stable.

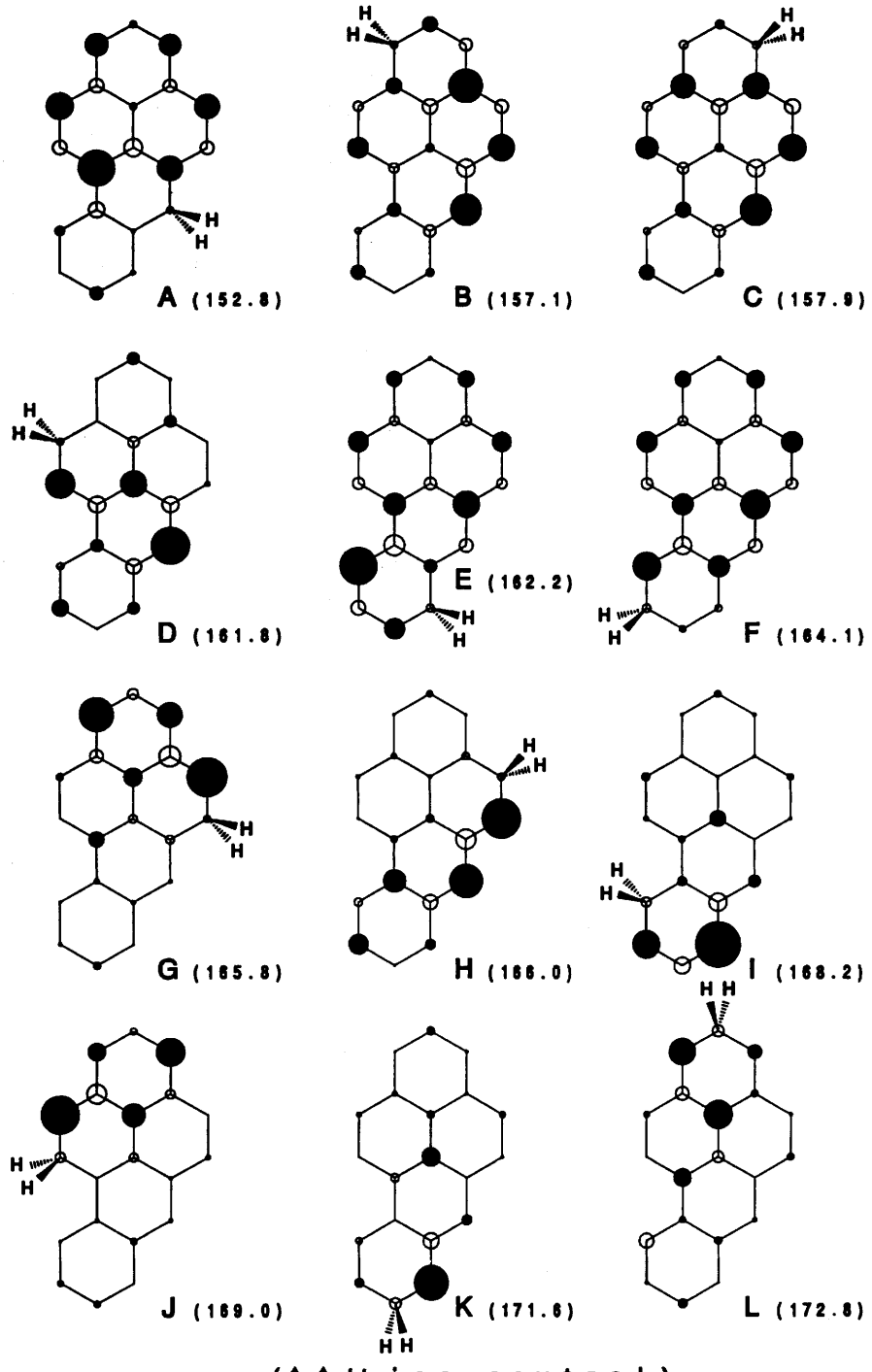

Fig. 5 AM1 calculated arenium ion energies ($\Delta\Delta H_f^\circ$) and ΔQ profiles for 1

A comparative discussion

The AM1 calculations and superacid protonation studies are in concert regarding the preference for C-6 protonation for **1** to generate the most stable arenium ion $\mathbf{1H}^+$. This finding is also consistent with the earlier theoretical (simple Hückel[31] and Dewar-PI[28]) predictions, the H–D exchange studies,[15] and the absorption spectrum of **1** in HF.[13,14] The δ_C *versus* charge relationship has been discussed for various classes of persistent carbocation.[27,32] Because ^{13}C chemical shifts are known to be determined largely by the charge density on the carbon, we have plotted $\Delta\delta_C$ *vs.* AM1 carbon charges (Fig. 10). The plot is roughly linear, but considerable scatter is observed. We note that the proton-bearing (empty symbols) and the quaternary carbons (filled symbols) seem to behave in the same manner. A number of points fall clearly to high $\Delta\delta_C$ values. These are from carbons close to the protonation site and are marked with c. Other chemical shifts are also perturbed. These are, *e.g.*, C-7a of $\mathbf{2H}^+$ and C-3b of $\mathbf{3aH}^+$ (marked with s) and the shifts could be due to steric hindrance caused by protonation. Several factors may be responsible: first, the absolute values of charges calculated by any quantum mechanical method are, to a greater or lesser extent, dependent on the assumptions and parametrisation of the method. Secondly, the calculated charges are for a gas-phase ion for which C–C and C–H polarisation is the

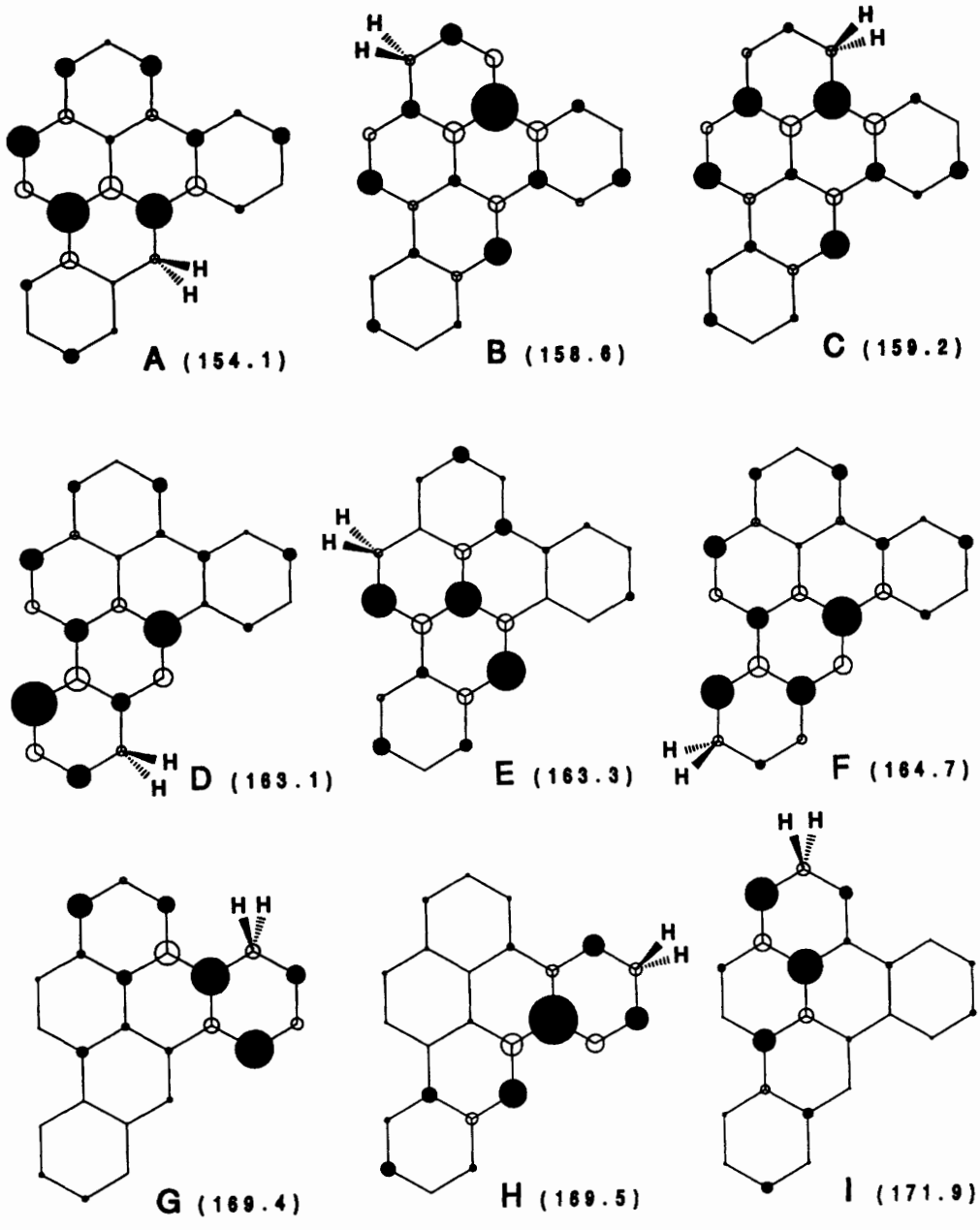

Fig. 6 AM1 calculated energies ($\Delta\Delta H_f^\circ$) and ΔQ profiles for **2**

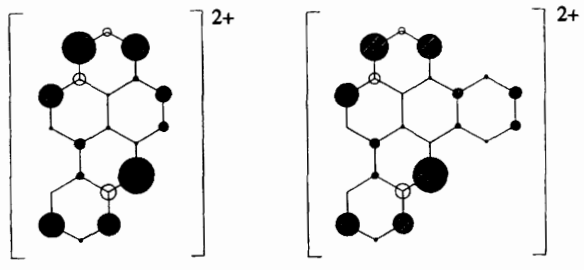

Fig. 7 ΔQ profiles (and $\Delta\Delta H_f^\circ$) for $\mathbf{1}^{1+}$ and $\mathbf{2}^{2+}$

dominant stabilising factor as opposed to a solution-phase ion where solvent stabilisation of charge is important. Thirdly, ring current anisotropy changes are not taken into account in a simple relationship with charges.[32a]

NMR studies reveal that the charge distribution pattern in $\mathbf{1H}^+$ remains analogous to pyrenium ions, showing a very distinct phenalenium cation moiety with little delocalisation of positive charge into the benzannellated ring. Charge alternation at the pyrene periphery and the phenalenium ion character are also predicted by AM1 calculations.

The least stable of the arenium ions formed by protonation at the β position of the pyrene moiety shows a very limited delocalisation path. This may be the driving force for α protonation which generates the most extensive charge alternation circuit *via* a robust phenalenium ion moiety.‡

‡ For previous studies of phenalenium cations see: R. J. Smith, T. M. Miller and R. M. Pagni, *J. Org. Chem.*, 1982, **47**, 4181. For synthesis of phenalenium cation salts and HMO calculations (RE = 5.83 β) see D. H. Reid, *Q. Rev. Chem. Soc.*, 1965, 274.

Relief of buttressing due to protonation is clearly evident by a comparison of $\Delta\delta$ values in the ^{1}H NMR spectra of $\mathbf{1H^+}$ with **1** and $\mathbf{2H^+}$ with **2**. In the latter, the effects at H-7, H-9, H-12 and H-13 are −0.64, −0.60, −0.58 and −0.09 ppm, respectively, whereas in $\mathbf{1H^+}$ the corresponding effects at H-5, H-7, H-10 and H-11 are −0.11, 0.01, −0.16 and −0.13 ppm.

Oxidation (→RC) remains a minor competing pathway which contributes to proton line-broadening and possibly also to chemical shift variations in the NMR spectra.

A comparison of protonation shifts for both ^{1}H and ^{13}C NMR spectra, taking into account the AM1 charges, illustrates that whereas the NMR data for $\mathbf{2H^+}$ can be constructed from those of $\mathbf{3aH^+}$ and the data for the benzene ring of $\mathbf{1H^+}$, the use of data for $\mathbf{1H^+}$ and the benzene ring of $\mathbf{3H^+}$ is not feasible.

It is also apparent that based on both AM1 charges and the $\Delta\delta_C$ data, the positive charge on the remote α positions of the pyrene moiety is larger in $\mathbf{1H^+}$ than in $\mathbf{2H^+}$, $\mathbf{3aH^+}$ and $\mathbf{3bH^+}$.

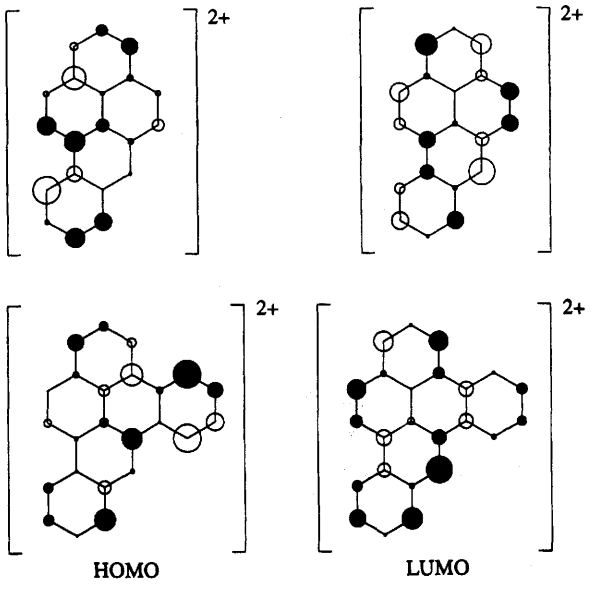

Fig. 8 The forms of the HOMO–LUMO for $\mathbf{2}^{2+}$ and $\mathbf{1}^{2+}$

The presence of the annellated ring leads to charge reduction at the annellated carbons by delocalisation into the annellated ring. Another interesting feature is that the preferred protonation site is always an α position of pyrene moiety which (except for $\mathbf{3bH^+}$) is always *peri* to either one ($\mathbf{1H^+}$), or two ($\mathbf{2H^+}$, $\mathbf{3bH^+}$) benzannellated ring(s), thus providing maximum relief of steric strain.

The total deshieldings (expressed by the sum of $\Delta\delta$ values) are close to 180 ppm for all four cations, supporting the monoarenium ion structure.

Relevance to carcinogenicity (Fig. 11)

We find that charge distribution pattern in the most stable arenium ions of **1** (a potent carcinogen), **2** (a mild carcinogen) and **3** (not a carcinogen) are rather similar, all showing extensive delocalisation into the pyrene moiety, exhibiting phenalenium ion character.

Metabolically, if a direct carbocation formation model is to be considered (attack by electrophilic oxygen), the regiospecificity of DNA binding (→carcinogenicity) must

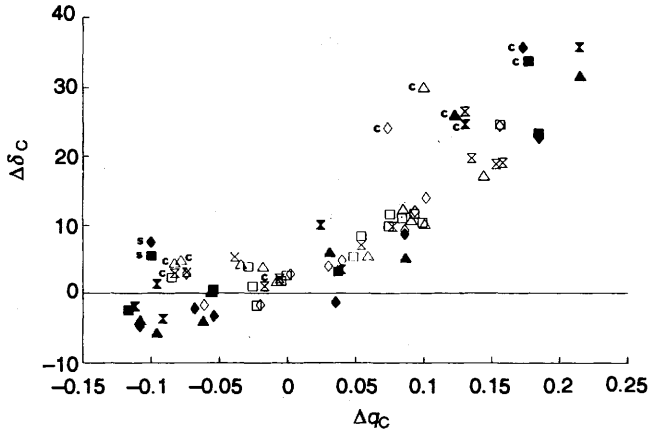

Fig. 10 Plot of $\Delta\delta_C$ chemical shifts *vs.* AM1 carbon charges: quaternary carbons are marked with filled symbols; c means close; s means steric (see the text); ⧖ $\mathbf{1H^+}$, □ $\mathbf{2H^+}$, ◇ $\mathbf{3aH^+}$, △ $\mathbf{3bH^+}$

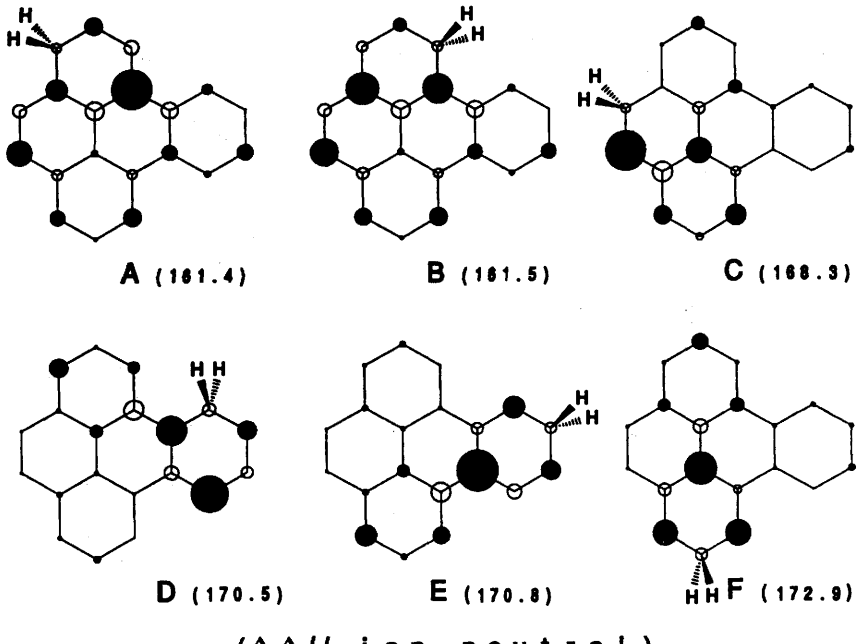

Fig. 9 AM1 energies ($\Delta\Delta H_f^\circ$) and ΔQ profiles for arenium ion of **3**

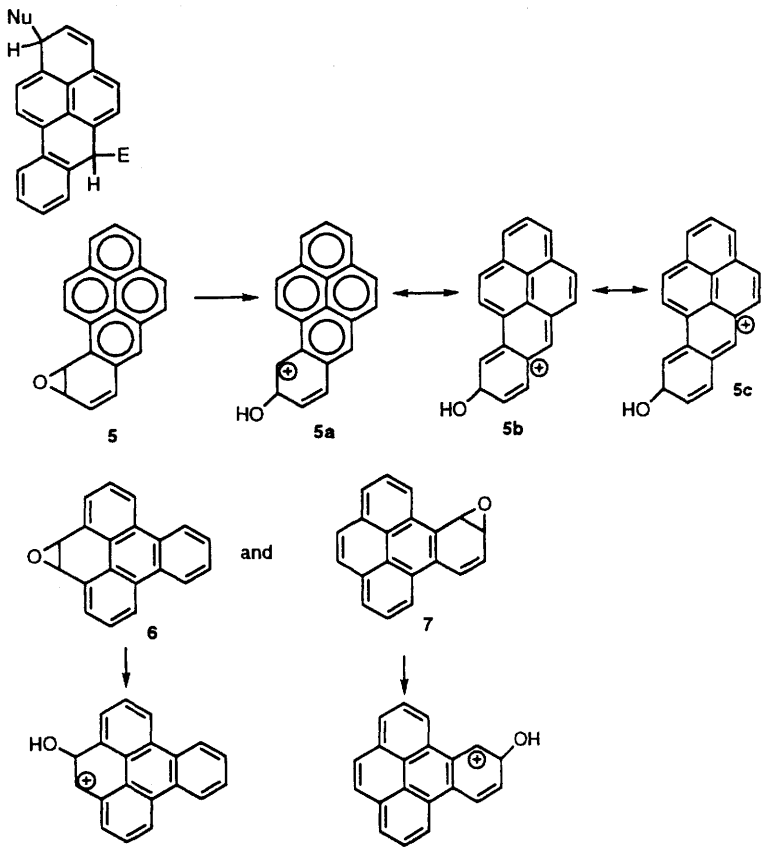

Fig. 11 Carbocation formation by direct electrophilic attack followed by remote nucleophilic attack, and the epoxide ring opening model to form carbocations

depend greatly on steric crowding at the most electrophilic sites of the arenium ion, and the availability of various nucleotides on DNA to bind with these positions. It has been shown[33] that under anodic oxidation, the RC of **1** was attacked by pyridine at C-6 whereas nucleophilic attack by 1-methylimidazole occurred at a remote site (C-1).

If, on the other hand, carbocations are produced by epoxide ring opening, as in **5**, this leads to benzylic/allylic carbocations for which mesomeric phenalenium ions similar to those of $\mathbf{1H}^+$ can result.

For **3**, the initially formed arene oxides are **6** and **7**.[34] Epoxide ring opening in these cases produces benzylic carbocations coupled to a benzophenanthrene moiety and coupled to an αβ carbon of a pyrene, respectively, neither of which is as stable as the phenalenium ion.

We are continuing our studies directed towards mapping of charge distributions in arenium ions of other dibenzopyrenes as well as different classes of fused PAH including fluorinated analogues which have exhibited varied degrees of carcinogenic properties in metabolic studies.

Experimental

Benzo[*a*]pyrene **1**, benzo[*a*,*e*]pyrene **2** and benzo[*e*]pyrene **3** were supplied by Rütgersweke. The purity of each sample was checked by ^1H and ^{13}C NMR spectroscopy. FSO_3H (Allied) and CF_3SO_3H (Aldrich) were distilled under argon in an all-glass distillation unit. SbF_5 (Flurochem) was freshly distilled under argon prior to use. Preparation of $FSO_3H{\cdot}SbF_5$ superacid systems has been described before.[22] SO_2ClF (Aldrich) was used without further purification.

AM1 Calculations were carried out at University of Akron using MOPAC 93 version running under OS/2. NMR Spectra were recorded on a GE-GN 300 MHz at KSU and a Bruker AC-250 MHz at Roskilde.

EPR spectrum of $2^{+\cdot}$

A cold aliquot of the superacid solution was transferred *via* a cold pipette (SO_2ClF) into a quartz EPR tube at dry ice–acetone temperature. The sample was repeatedly flushed with argon and sealed. The X-band EPR spectrum was obtained at 210 K using an IBM 200D-SRC spectrometer with an ER 4111 temperature controller with 1K precision. The unresolved hyperfine coupling did not improve by lowering the temperature or by sealing the sample after a freeze–thaw cycle.

Preparation of the stable ions

Typically, 25–28 mg of the substrate was placed in a 10 mm NMR tube, slurried in *ca.* 1 cm^3 of SO_2ClF under argon, and the tube was cooled in a dry ice–acetone bath. The superacid (*ca.* 1 cm^3) was placed in a second 10 mm NMR tube and was diluted with *ca.* 1 cm^3 of SO_2ClF (efficient vortex mixing). The precooled acid was slowly poured into the substrate under argon at dry ice–acetone temperature with efficient (vortex) mixing, whereupon a red homogeneous solution was formed. A cold aliquot was transferred directly to a 5 mm NMR tube fully immersed in the dry ice–acetone bath. Precooled CD_2Cl_2 (8–10 drops) was added (vortex mixing) and the sample was examined by NMR spectroscopy within 1–2 h of preparation. The ions proved to be quite stable and cold samples stored for several days were found to be unchanged (NMR).

Acknowledgements

We thank NATO for a research travel grant (CRG. 930113), KSU and Roskilde University for partial support and the Ohio

Academic challenge program for the purchasing funds for our GE-GN 300 MHz instrument. We are grateful to Dr. Edward Gelerinter (KSU Physics Dept.) for the EPR work.

References

1 R. G. Harvey, *Polycyclic Aromatic Hydrocarbons: Chemistry and Carcinogenicity*, Cambridge University Press, Cambridge, UK, 1991.
2 W. Levin, A. Wood, R. Chang, D. Ryan, P. Thomas, H. Yagi, D. Thakker, K. Vyas, C. Boyd, S.-Y. Chu, A. Conney and D. Jerina, *Drug Metabol. Rev.*, 1982, **13**, 555.
3 R. E. Lehr, S. Kumar, W. Levin, A. W. Wood, R. L. Chang, A. H. Conney, H. Yagi, J. M. Sayer and D. M. Jerina, 'The Bay Region Theory of Polycyclic Aromatic Hydrocarbons Carcinogenesis' in *Polycyclic Hydrocarbons and Carcinogenesis*, ACS Symposium Series 283, pp. 63–84, ed. R. G. Harvey, American Chemical Society, Washington DC.
4 Review: F. P. Guengerich, *Pharmacol. Ther.*, 1992, **54**, 17.
5 P. Cremonesi, B. Hietbrink, E. G. Rogan and E. L. Cavalieri, *J. Org. Chem.*, 1992, **59**, 3309; see also ref. 3.
6 E. L. Cavalieri, P. D. Devanesan, P. Cremansi, S. Higginbatham and E. G. Rogan in *Polynuclear Aromatic Hydrocarbons: Measurements, Means and Metabolism*, eds. M. Cooke, K. Loening and J. Merritt, Battelle Press, Columbus, 1991.
7 N. V. S. RamaKrishna, E. L. Cavalieri, E. G. Rogan, G. Dolnikowski, R. L. Cerny, M. L. Gross, H. Jeang, R. Jankowiak and G. L. Small, *J. Am. Chem. Soc.*, 1992, **114**, 1863.
8 N. T. Nashed, J. M. Sayer and D. M. Jerina, *J. Am. Chem. Soc.*, 1993, **115**, 1723.
9 N. T. Nashed, A. Bax, R. J. Lancharich, J. M. Sayer and D. M. Jerina, *J. Am. Chem. Soc.*, 1993, **115**, 1711.
10 T. C. Bruice and P. Y. Bruice, *Acc. Chem. Res.*, 1976, **9**, 378.
11 M. D. Johnson and M. Calvin, *Nature (London)*, 1973, **241**, 271.
12 G. Dallinga, E. L. Mackor and A. A. Verrijn-Stuart, *Mol. Phys.*, 1958, **1**, 123.
13 C. MacLean, J. H. Van der Waals and E. L. Mackor, *Mol. Phys.*, 1958, **1**, 247.
14 H.-H. Perkampus in *Advances in Physical Organic Chemistry*, ed. V. Gold, Academic Press, 1966, Vol. 4, pp. 195–304.
15 E. Cavalieri and M. Calvin, *Proc. Nat. Acad. Sci. USA*, 1971, **68**, 1251.
16 K. K. Laali and P. E. Hansen, *J. Org. Chem.*, 1991, **56**, 6795.
17 K. K. Laali, T.-M. Liang and P. E. Hansen, *J. Org. Chem.*, 1992, **57**, 2658.
18 K. K. Laali, P. E. Hansen, E. Gelerinter and J. J. Houser, *J. Org. Chem.*, 1993, **58**, 4088.
19 K. K. Laali and P. E. Hansen, *J. Org. Chem.*, 1993, **58**, 4096.
20 K. K. Laali, *J. Chem. Soc., Perkin Trans. 2*, 1993, 1873.
21 K. K. Laali and J. J. Houser, *J. Chem. Soc., Perkin Trans. 2*, 1993, 1303.
22 K. K. Laali and P. E. Hansen, *J. Chem. Soc., Perkin Trans. 2*, 1994, 2249.
23 K. K. Laali, P. E. Hansen and S. Bolvig, *J. Chem. Soc., Perkin Trans. 2*, 1995, 537.
24 C. J. Unkefer, R. E. London, T. W. Whaley and G. H. Daub, *J. Am. Chem. Soc.*, 1983, **105**, 733.
25 R. Bunte, Thesis, Clausthal, Germany, 1986.
26 C. J. Pauchart and J. Behnke, *The Aldrich Library of ^{13}C and ^{1}H FT-NMR Spectra*, Aldrich Chemical Company, edn. 1, vol. 2, 1993.
27 D. A. Forsyth and G. A. Olah, *J. Am. Chem. Soc.*, 1976, **98**, 4036.
28 V. Gold and F. L. Tye, *J. Chem. Soc.*, 1952, 2184.
29 M. J. S. Dewar and R. D. Dennington II, *J. Am. Chem. Soc.*, 1989, **111**, 3804.
30 M. J. Rioseras-Garcia and J. M. Hernando-Huelme, *J. Org. Chem.*, 1994, **59**, 2135.
31 A. G. Davies and C. J. Shields, *J. Chem. Soc., Perkin Trans. 2*, 1989, 1001.
32 (*a*) B. Eliasson, D. Johnels, I. Sethson, U. Edlund and K. Müllen, *J. Chem. Soc., Perkin Trans. 2*, 1990, 897; (*b*) G. K. S. Prakash, T. N. Rawdah and G. A. Olah, *Angew. Chem., Int. Ed. Engl.*, 1983, **22**, 390; (*c*) G. A. Olah, G. K. S. Prakash and J. Sommer, *Superacids*, Wiley, New York, 1985, ch. 3.
33 G. M. Blackburn and J. P. Will, *J. Chem. Soc.*, 1974, 67.
34 S. K. Agrawal, D. R. Boyd, R. Dunlop and W. B. Jennings, *J. Chem. Soc., Perkin Trans. 1*, 1988, 3013.

Paper 5/01774B
Received 21*st March* 1995
Accepted 11*th May* 1995